Bull. Mater. Sci., Vol. 37, No. 6, October 2014, pp. 1509–1514. © Indian Academy of Sciences.

Influence of Be doping on the characteristics of CdO/p-Si heterojunction for optoresponse applications

A A DAKHEL

Department of Physics, College of Science, University of Bahrain, P.O. Box 32038, Kingdom of Bahrain

MS received 10 November 2013

Abstract. In this work, the optoelectronic properties of Be-doped CdO films grown on p-Si forming CdO : Be/p-Si hetero-p–n junctions were investigated. The spotlight was on the influence of electronic properties of CdO : Be layers, which were controlled by Be-dopant content, on the optoelectronic properties of the constructed p–n heterojunction. The characterization of the transparent conducting oxide CdO : Be layer was performed with X-ray diffraction, scanning electron microscopy, electrical measurements and spectral photometry. It was found that Be doping greatly enhanced the optoresponse (S^*) of the p–n heterojunction, such that S^* was boosted by ~36 times for CdO : 0·10% Be/p-Si sample, compared with the undoped CdO/p-Si. This S^*-enhancement was explained by the improvement of carrier mobility in host CdO with Be doping. Therefore, the utmost S^* that was found with 0·10% Be-doped CdO sample was due to its highest carrier mobility among other samples of different Be content. The results of optoelectronic measurements in visible and NIR spectral range demonstrate the utility of the CdO : Be/p-Si heterojunction in photodetection applications.

Keywords. Cd–Be oxide; Be-doped CdO; CdO : Be/Si heterojunction; photoresponsivity.

1. Introduction

The optoelectronic properties of transparent conducting oxides (TCOs) could be controlled through controlling their intrinsic natural structural point donor defects such as metal interstitials (M_i) and oxygen vacancies (V_o). Doping of TCOs by foreign ions is the foremost method that can be used to manage and develop the optoelectronic properties for TCO films that are used in devices production, like flat panel displays and solar energy systems (Calnan and Tiwari 2010). CdO is one of the TCOs that has a good transparency in the visible and NIR spectral regions with a direct bandgap of 2·2–2·7 eV (Carballeda-Galicia *et al* 2000; Zhao *et al* 2002). The conductivity of CdO films is being in the range of 10^2–10^4 S/cm and that could be improved with doping by different suitable metallic ions like Y, In, Sm, etc. (Dou *et al* 1998; Asahi *et al* 2002; Dakhel 2009). Especially, doping of CdO films with small size ions (compared to that of Cd^{2+} ion of radius $9{\cdot}5 \times 10^{-2}$ nm (Shannon 1976) like Cr, W, Ge and B could effectively improve the carrier mobility as well as the conductivity (Dakhel 2012; Dakhel and Hamad 2012). Furthermore, doping can create in CdO films exotic properties, such as magnetic and photosensation that makes the study of doped CdO useful and fruitful. p–n heterojunctions based on metallic oxide films deposited on silicon layers are usually used as elements for construction of optoelectronic devices. Properties of CdO/Si heterojunction were studied recently in Yakuphanoglu (2010) for undoped CdO and Murali *et al* (2010), Dakhel (2011), Karatas and Yakuphanoglu (2012), Farag *et al* (2012) for doped CdO with Al, B, Cu and Zn. In the present study, Be-doped CdO thin films grown on p-Si substrates (CdO : Be/p-Si) forming p–n heterojunctions were investigated focusing on the influence of Be doping on the optoelectronic properties of the heterojunction, through its effect on the carrier mobility.

2. Experimental

Be-doped CdO thin films were prepared by reactive vacuum evaporation method in a chamber of residual oxygen atmosphere of about $1{\cdot}3 \times 10^{-3}$ Pa. The substrates used were ultrasonically cleaned glass slides and chemically (using 48% HF) cleaned shiny *p*-type ($1{\cdot}89 \times 10^{15}$ cm^{-3}) silicon wafers of ⟨1 0 0⟩ orientation (Wafer World Inc., FL, USA). The alternative evaporation method (layer-by-layer) of the starting materials (pure Be and CdO from Fluka A.G./Germany) by using alumina baskets (Midwest Tungsten Service, USA) was used. The as-deposited films were flash annealed in air at 400 °C for 1 h. The evaporated masses were controlled with a piezoelectric microbalance sensor (Philips FTM5) while the film thicknesses were measured after annealing by an MP100-M spectrometer (Mission Peak Optics Inc., USA), to be

(adakhil@uob.edu.bh)

0·2–0·3 μm. Six sets of CdO : Be films were prepared, each set has different wt% of Be dopant that was measured with a scanning electron microscope, SEM (SEM/EDX microscope Zeiss EVO) to be about 0·06%, 0·08%, 0·10%, 0·11%, 0·12% and 0·13% (each film sample was referred by its Be% content). The structure of the samples was investigated by the X-ray diffraction (XRD) (Philips PW 1710) method using CuKα line. The normal absorbance $A(\lambda)$ of the samples was measured in UV–Vis–NIR spectral region (300–3000 nm) on a Shimadzu UV-3600 double beam spectrophotometer. For electrical measurements, gold films of around 200 nm were deposited forming gate contact to each Au/CdO : Be/p-Si device. The measurements of conductivity and mobility of Be-doped CdO films were performed with a standard four-probe method. The *I–V* electrical measurements were carried out on Au/CdO : Be/p-Si samples by using a Keithley model 6487 pico-ammeter.

3. Structural, optical and electrical characterization

The normalized XRD patterns of the prepared pure and Be-doped CdO films are shown in figure 1. They reveal that all the investigated films are cubic of *Fm*3*m* CdO structure with a lattice parameter of around 0·469 nm, which is close to the standard value (JCPDS file no. 05-0640). The energetically preferred (1 1 1) orientation of the undoped CdO film keep on with Be-doped CdO films. As clear from the normalized patterns, the Be doping strengthened the (1 1 1) orientation growth over other reflections like (2 0 0), so that 0·10% Be film became almost singly (1 1 1) oriented, compared to the polycrystalline undoped CdO film prepared under the same conditions.

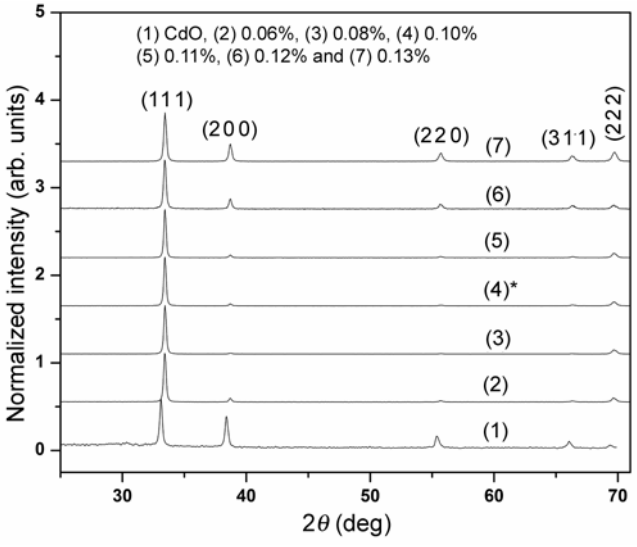

Figure 1. X-ray diffraction patterns for pure and Be-doped CdO films.

With increasing Be content over 0·1%, the (1 1 1) orientation gradually weakened referring to structural gradual degradation. Generally, the XRD patterns show no peaks related to Be or its oxide phase, which implies that incorporated Be^{2+} ions were dissolved in the lattice of CdO. However, the incorporation of small size Be^{2+} ions in the interstitial sites (Be_i) of lattice structure of CdO disturbs the charge equilibrium of the unit cell that should be settled by creation of Cd^{2+} ion vacancies (V_{Cd}) and/or formation of interstitial oxygen (O_i). Furthermore, some of Be^{2+} ions that occupied interstitial positions might move by thermal motion for occupying Cd^{2+}-ion vacancies resulting in Be_{Cd} which referes to the formation of a substitutional solid solution (or SSS-type).

The mean X-ray crystallite size (CS) can be estimated by using Scherrer's equation (Kaelble 1967) to be ~ 35 nm for undoped CdO film that slightly increased to 38–42 nm with Be incorporation. This implies that the samples are nanocrystallites.

The SEM study shows morphological variations in the CdO films because of Be doping. Figure 2 shows scanning electron micrographs for (a) undoped CdO, (b) 0·06%, (c) 0·10% and (d) 0·12% Be-doped CdO samples. It can be seen that pure CdO film has a woolly-shaped elements, which were converted into almost round grains of size (GS) ~ 60, 120 and 80 nm for 0·06%, 0·10% and 0·12% samples, respectively.

The spectral absorbance $A(E)$ of the prepared films in the UV–Vis–NIR spectral region for the prepared films are depicted in figure 3. The bandgaps E_g of the films were evaluated by using Hamberg *et al* (1984) relation

$$A(E) = A_0\left[1 - \frac{2}{\pi}\tan^{-1}\left(\frac{E_g - E}{\Gamma}\right)\right] + A_1, \quad (1)$$

where A_0 and A_1 are the fitting constants, Γ the parameter that account for the broadening of the initial and final states caused by electron scattering ($\Gamma < 1$ eV). Fitting of the obtained experimental data to (1) in the band-to-band absorption energy region is shown in figure 3 and yields the values of E_g that are shown in figure 4. The obtained bandgap (2·53 eV) of undoped CdO agrees with the range (2·2–2·7 eV) known for CdO films prepared by different methods. The bandgap of host CdO slightly shrinks by ~ 4% with light (0·1%) Be doping, after which a sudden decrease by about 24 with 0·13% Be doping happens.

4. Electrical properties of CdO : Be/p-Si heterojunction

The *I–V* characteristics of undoped and Be-doped CdO/p-Si samples measured in dark (a) and under illumination by incandescent lamp light (b), are shown in figure 5(a) and (b). For the first observation, weak diode effect that

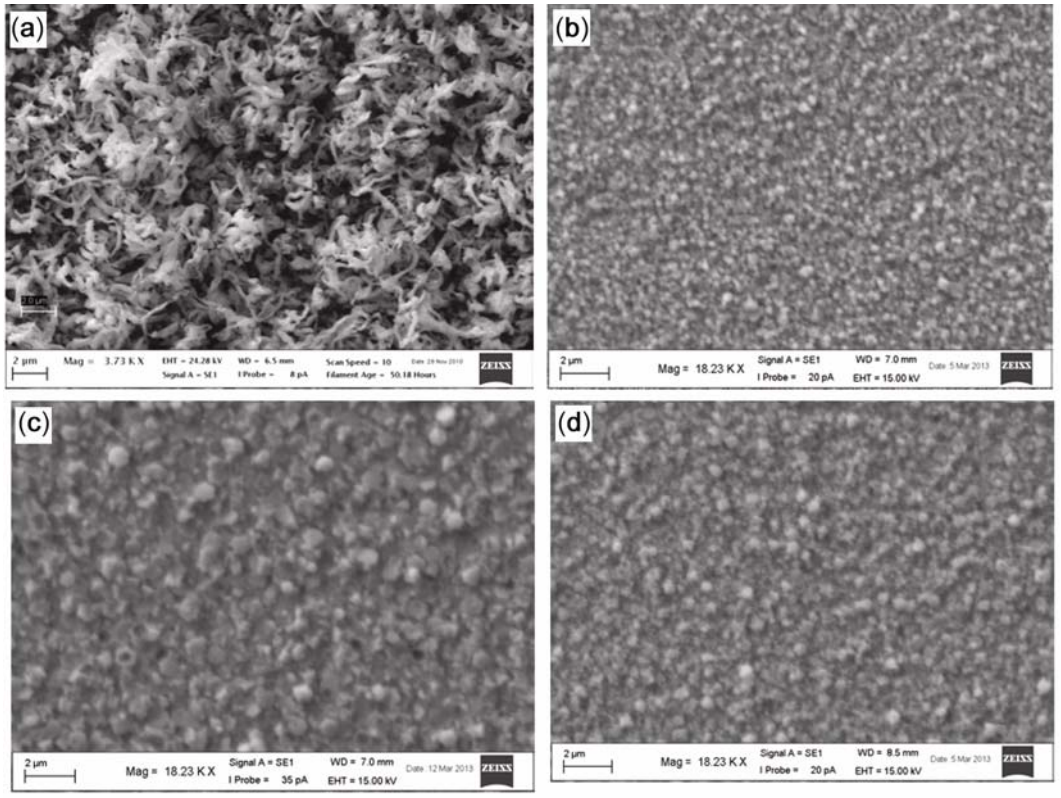

Figure 2. Scanning electron micrographs for (**a**) undoped, (**b**) 0·06%, (**c**) 0·10% and (**d**) 0·12% Be-doped CdO films.

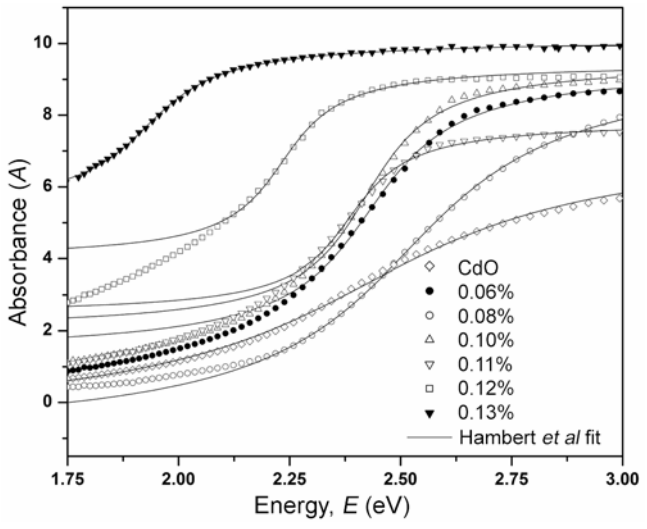

Figure 3. Spectral absorbance points for undoped and Be-doped CdO films deposited on glass substrates. The fitting lines according to Hamberg *et al* (1984) are shown.

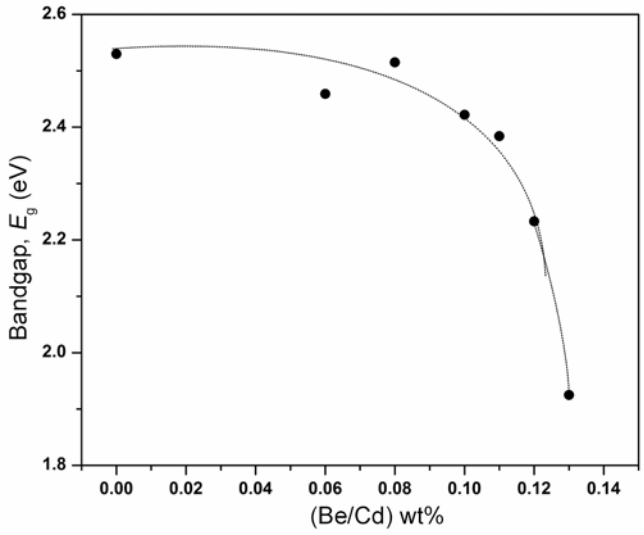

Figure 4. Be-content dependence of Hamberg *et al* (1984) bandgap of CdO : Be films.

was measured in dark conditions almost totally disappeared under illumination. The well-known thermoionic emission (TE) theory that describes the $I_F - V$ relation in forward direction is used to analyse the experimental results of figure 5(a) (Sze 2002). The calculated effective potential barrier height (BH) at p–n junction at zero applied voltage (ϕ_{B0}) as a function of Be% content in CdO is shown in figure 6. The result shows that the Be doping has complicated effect on the value of ϕ_{B0}. It can be seen that with increasing of Be% content, the value of BH decreases until the doping level of 0·08–0·10%, after which it increased asymptotically to certain value close to

that of undoped CdO/p-Si. This can be explained by the structural variations including GS in CdO:Be film. For Be-doping level larger than 0·1%, some of the incorporated Be-dopant oxide starts to accumulate on crystallite and grain boundaries including the CdO/Si interface region causing increase in BH (figure 6) In general, the structural variations in CdO layer caused by Be doping influence and control the value on ϕ_{B0}.

The current flow through the constructed p–n heterojunctions is controlled mainly by the interface layer properties especially for low voltages and the CdO layer properties for higher voltages. Among many types of mechanisms that control the d.c. current flow in insulators and semiconductors, the space-charge-limited current (SCLC) is considered (Sze 1981; Dakhel 2006). According to the SCLC mechanism, the I–V characteristics are described by $I \sim V^s$, where s is $n = 2$ for usual SCLC mechanism, and $n > 2$ for trap-charge-limited conductivity (TCLC) mechanism. Figure 7 shows the dependence of the current on the forward voltage ($V_F > 1$ V) in log–log scale for Be-doped CdO films. The behaviours show that the Be-doped CdO/p-Si samples of 0·06%, 0·08%, 0·10%, 0·11% and 0·12% follow the SCLC mechanism. However, sample 0·13% follows TCLC that might be due to the effect of mixed phases: CdO : Be with amorphous Be–Cd oxide accumulated on CBs and GBs.

The electrical conductivity and mobility of Be-doped CdO films were measured with four-probe method. The utmost conductivity ($2{\cdot}42 \times 10^3$ S/cm) and mobility (129 cm^2/V s) was found with CdO film doped with 0·1% Be. The variation of conductivity and mobility with Be% content is shown in figure 8.

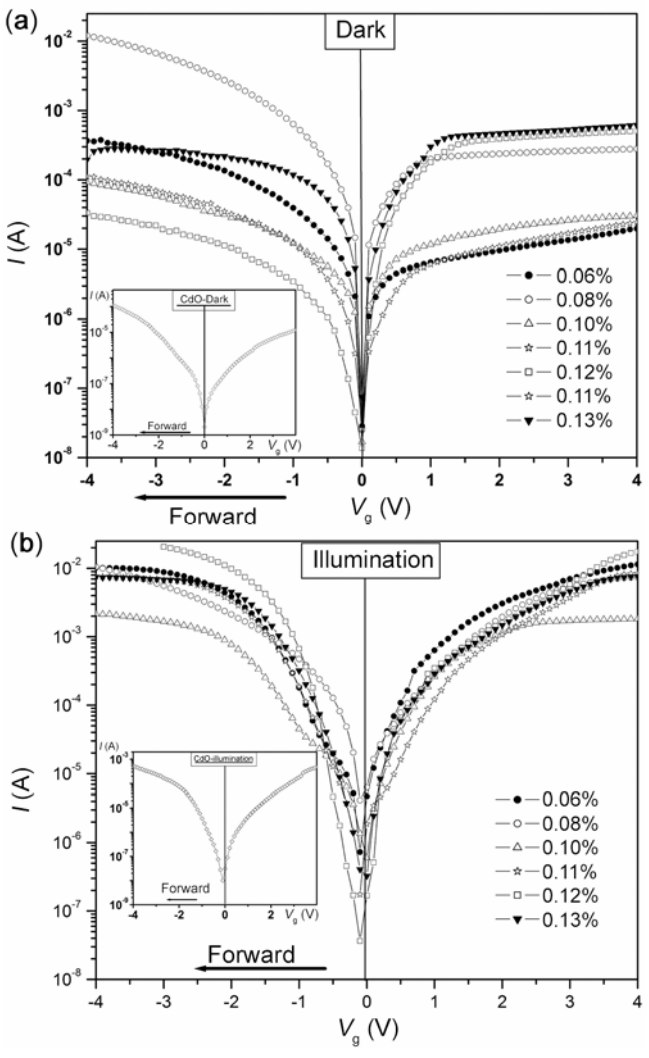

Figure 5. Current–voltage dependence for the constructed Au/CdO : Be/p-Si heterojunction: (**a**) in dark and (**b**) under illumination.

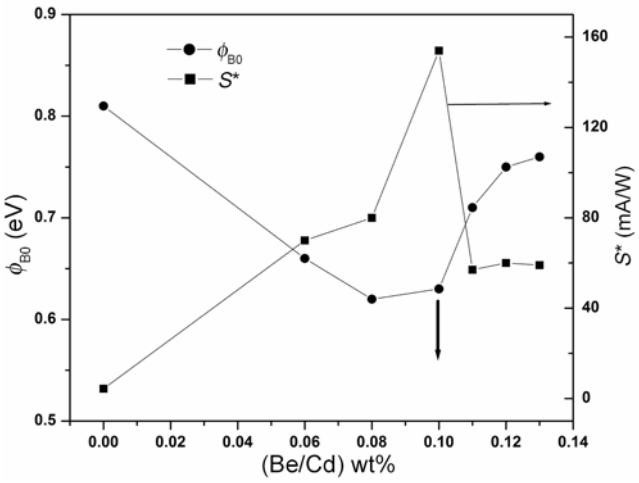

Figure 6. Comparison of the Be%-dopant dependence of barrier height (ϕ_{B0}) and optoresponse (S^*) of Au/CdO : Be/p-Si heterojunctions.

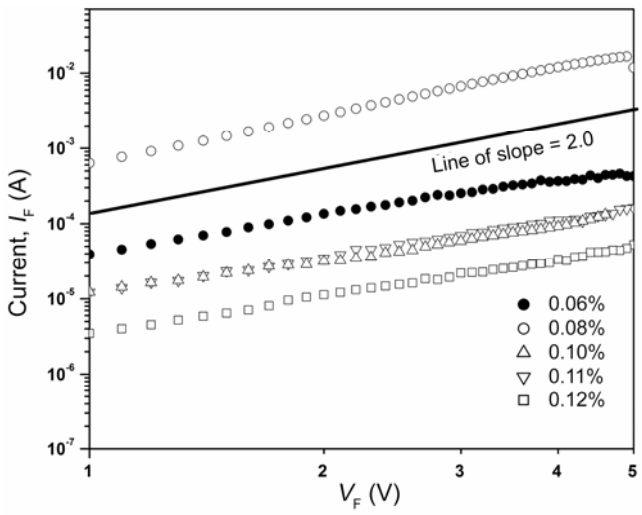

Figure 7. Forward I–V characteristics following SCLC mechanism for Be-doped CdO/p-Si.

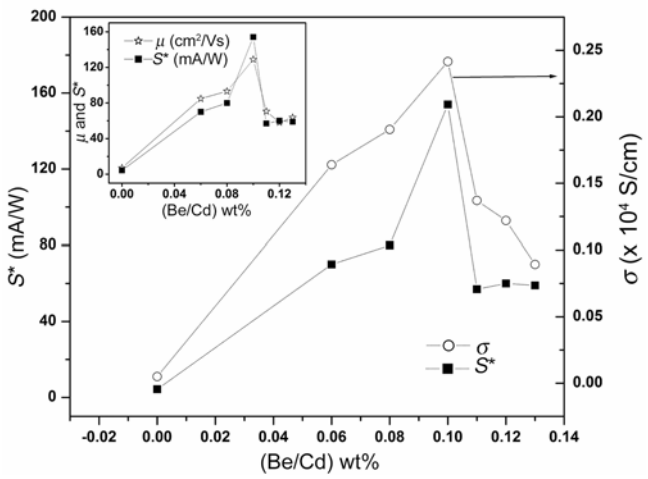

Figure 8. Comparison of the Be-content dependence of host CdO film conductivity and optoresponse (S^*) of Au/CdO : Be/p-Si heterojunctions. The inset shows a comparison of the Be-content dependence of host CdO film carrier mobility and optoresponse of that heterojunctions.

5. Optoelectronic measurements

The optoelectronic properties of the constructed CdO : Be/p-Si heterojunctions were investigated under illumination of incandescent lamp light of maximum intensity at 630 nm and integral intensity of 26·6 mW/cm^2. The optoresponse (mA/W) is defined as $S^* = (I_l - I_d)/E_{in}$, where I_l and I_d are the currents measured at +2 V under light illumination and in dark, respectively, and E_{in} is the incident illumination energy. The optoresponse depends on the CdO/Si interface state as well as the optoelectronic properties of the CdO : Be layer. Thus, it should be expecting some relationship between S^* and BH, conductivity and carrier mobility in CdO : Be layer. The comparison of the Be-content dependent of S^* and BH is shown in figure 6, where one can observe the opposite dependence behaviour. The Be-content dependences of S^*, conductivity and carrier mobility of CdO : Be film are shown in figure 8, where one can observe the similar behaviour of dependences. Therefore, the electrical properties of host CdO control the photoresponse of the heterojunction. The utmost optoresponse (154 mA/W) is obtained with 0·10% Be-doped CdO layer. (This layer has the highest conductivity, highest mobility, largest grain size and strongest [1 1 1] orientation among the studied layers of different Be content.) The utmost optoresponse might be related to utmost carrier mobility. So, according to the Einstein–Smoluchowski relation, the diffusion length (L) is related to the carrier mobility by

$$L = (D \cdot \tau)^{1/2} = (k_B T \mu \tau / e)^{1/2} \sim \mu^{1/2},$$

where D is the diffusion coefficient at temperature T and τ the carrier lifetime. Thus, higher mobility in CdO : Be layer causes higher diffusion length (L) or longer lifetimes (τ) that is responsible for higher optoresponse. To compare the present results with other photosensitive p–n heterojunctions; the following experimental results are mentioned. The photoresponse of undoped CdO film, prepared by sol–gel method on p-Si heterojunction, was measured by using a white light source to be ~ 22 mA/W per unit area (cm^2) (Yakuphanoglu *et al* 2010). For p-ZnO/n-Si, the photoresponse was 204 mA/W at 530 nm (Chen 2012). Furthermore, it was recorded that the photoresponse of ZnO/Si heterojunction at 420 nm was increased from 10 to 220 mA/W by doping of ZnO with Al (Dzhafarov *et al* 2010). In addition, it was found (Dzhafarov *et al* 2010) that doping of indium to n-CdS grown on p-Si causes increase of the responsivity from about 200 to 700 mA/W for 700 nm.

6. Conclusions

It was established that the optoelectronic properties of CdO layer can be controlled by Be-doping. Furthermore, such doping also controls the optoelectronic properties of the p–n heterojunctions based on CdO : Be layer deposited on p-Si substrate. A good optical response value ~ 154 mA/W was recorded by utilizing 0·10 wt% Be-doped CdO layer. These results show that CdO : Be/p-Si heterojunctions act as a good candidate for the production of photodetectors.

References

Asahi R, Wang A, Babcock J R, Edleman N L, Metz A W, Lane M A, Dravid V P, Kannewurf C R, Freeman A J and Marks T J 2002 *Thin Solid Films* **411** 101

Calnan S and Tiwari A N 2010 *Thin Solid Films* **518** 1839

Carballeda-Galicia D M, Castanedo-Pérez R, Jiménez-Sandoval O, Jiménez-Sandoval S, Torres-Delgado G and Zúñiga-Romero C I 2000 *Thin Solid Films* **371** 105

Chen L-C 2012 *Si-based ZnO ultraviolet photodiodes, photodiodes – from fundamentals to applications* (ed.) Ilgu Yun ISBN: 978-953-51-0895-5, InTech, DOI: 10.5772/48825. Available from: http://www.intechopen.com/books/photodiodes-from-fundamentals-to-applications/si-based-ZnO-ultraviolet-photodiodes

Dakhel A A 2006 *J. Alloys Compd.* **416** 17

Dakhel A A 2009 *J. Alloys Compd.* **475** 51

Dakhel A A 2011 *Curr. Appl. Phys.* **11** 11

Dakhel A A 2012 *J. Electron. Mater.* **41** 2405

Dakhel A A and Hamad H 2012 *Int. J. Thin Films Sci. Technol.* **1** 25

Dou Y, Egdell R G, Walker T, Law D S L and Beamson G 1998 *Surf. Sci.* **398** 241

Dzhafarov T D, Ongul F and Yuksel S A 2010 *Vacuum* **84** 310

Farag A A M, Cavas M and Yakuphanoglu F 2012 *Mater. Chem. Phys.* **132** 550

Gupta B, Jain A and Mehra R M 2010 *J. Mater. Sci. Technol.* **26** 223

Hamberg I, Granqvist C G, Berggren K F, Sernelius B E and Engstrom L 1984 *Phys. Rev.* **B30** 3240

JCPDS file no. 05-0640, Powder Diffraction File, Joint Committee for Powder Diffraction Studies

Kaelble E F 1967 *Handbook of X-rays for diffraction, emission, absorption, and microscopy* (New York, USA: McGraw-Hill) p 17

Karatas S and Yakuphanoglu F 2012 *J. Alloys Compd.* **537** 6

Murali K R, Kalaivanan A, Perumal S and Neelakanda Pillai N 2010 *J. Alloys Compd.* **503** 350

Shannon R D 1976 *Acta Crystallogr.* **A32** 751

Sze S M 1981 *Physics of semiconductor devices* (John Wiley & Sons Inc.) 2nd ed

Sze S M 2002 *Semiconductor devices: physics and technology* (New York: Wiley) vol. 4, 2nd ed

Yakuphanoglu F, Caglar M, Caglar Y and Ilican S 2010 *J. Alloys Compd.* **506** 188

Zhao Z, Morel D L and Ferekides C S 2002 *Thin Solid Films* **413** 203